Experimental report

16/02/2025

Proposal: 9-12-669 **Council:** 10/2022

Title: Self-assembly of multi-layered polyelectrolyte-surfactant coatings with long-lasting antimicrobial protection

Research area: Soft condensed matter

This proposal is a new proposal

Main proposer: Egor BERSENEV

Experimental team: Egor BERSENEV
Oleg KONOVALOV

Local contacts: Philipp GUTFREUND
Leonardo CHIAPPISI

Samples: polymer-surfactant complex

Instrument	Requested days	Allocated days	From	To
D17	3	0		
FIGARO	3	2	26/06/2023	28/06/2023
SUPERADAM	3	0		

Abstract:

We propose an neutron reflectivity combined with off-specular scattering study in collaboration with Procter & Gamble UK (the partner of InnovaXN project), the world leading manufacturer in personal care products, to study the spontaneous self-assembly of novel polymer-surfactant multilayer films. Our ultimate goal is to use such complex coatings to provide long-lasting antimicrobial properties for surfaces, without the need for constant sanitization. The design of the system is based on the concept that such longevity in antimicrobial efficacy may be offered by creating a multilayer coating with antimicrobial agents uniformly dispersed through the whole film, which can be released over a sustained period of time. We will study film structure to elucidate localisation of surfactants in the polymer matrix and effect of humidity on the solvent distribution inside the film in order to elucidate optimal composition for the sustained antimicrobial surface property.

Soft Matter

ARTICLE TYPE

Cite this: DOI: 00.0000/xxxxxxxxxx

Confined polymer-surfactant complexes spontaneously form stratified lamellar phase

Egor A. Bersenev,*[a,b] Phillip Gutfreund, [c] Rebecca J. Fong, [d] Oleg V. Konovalov,[b] and Wuge H. Briscoe[a]

Received Date
Accepted Date

DOI: 00.0000/xxxxxxxxxx

We investigated the structure of humidity responsive polymer-surfactant complexes of a hydrophilic maleic acid polymer and an amphoteric amine oxide surfactant (C12-AO) on the solid-air interface. Neutron reflectometry (NR) revealed the presence of a smooth nanofilm at the interface comprising several surfactant bilayers. Upon exposure to humidity, the nanofilm reorganized into a vertically stratified multilayer structure with polymer chains located in the vicinity of surfactant headgroups. Off-specular neutron reflectometry and grazing-incidence X-ray scattering revealed the presence of polydisperse pores in the nanofilm across several length scales. Finally, small angle X-ray scattering did not detect the presence of any polymer-surfactant lamellar aggregates in the solution, pointing to the role of the 2D confinement in the observed formation of the multilayer nanofilms.

1 Results

1.1 Out-of-plane structure of polymer-surfactant complex films

To determine the distribution of the surfactant in the spin-coated film perpendicular to the interface, two isotropic contrasts were investigated: h-polymer with h-surfactant, swollen with D_2O vapours; and h-polymer with d-surfactant, swollen with D_2O vapours. Visually, the spin-coated film was smooth and highly sensitive to the relative humidity, evident from its colour change from light yellow to deep blue upon humidity increase.

The presence of multiple Kiessig fringes in the low-q region in the NR profiles in dry N2 and under RH 27, 55, 80% and after drying (Figure 1) is consistent with a film with a well defined thickness, with a broad Bragg peak also present (Fig. 1A; indicated by small arrows), indicating the periodicity in the structure in the as-prepared film placed into the dry nitrogen atmosphere (RH=0%). For the films with d-surfactant (Fig. 1B), the critical edge in the NR profile was shifted to a higher q, indicating a higher average scattering length density (SLD), whilst the Bragg

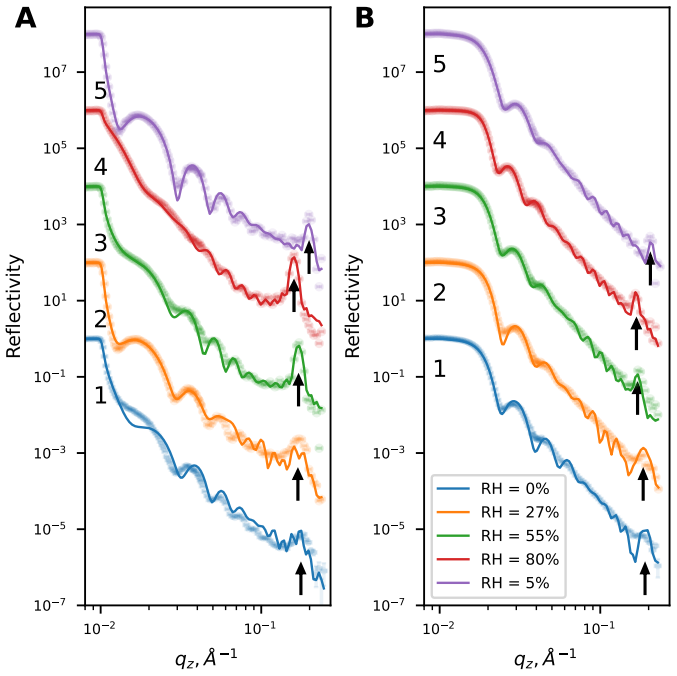

Fig. 1 Neutron reflectometry profiles. A. Film, containing h-surfactant; B. Films, containing d-surfactant. Thin solid lines represent fits to the models, described in the text. Arrows indicate the position of the Bragg peak for each curve. Curves are shifted two orders of magnitude for visibility and labelled 1 to 5 for clarity.

[a] School of Chemistry, University of Bristol, Cantock's Close, Bristol, BS8 1TS, United Kingdom
E-mail: egor.bersenev@bristol.ac.uk
[b] European Synchrotron Radiation Facility (ESRF), 71 avenue des Martyrs, 38000 Grenoble, France.
[c] Institut Laue–Langevin (ILL), 71 Avenue des Martyrs, 38000, Grenoble, France 38000, France.
[d] Procter&Gamble, Newcastle Innovation Centre, Newcastle upon Tyne NE12 9TS, United Kingdom

† Electronic Supplementary Information (ESI) available: [details of any supplementary information available should be included here]. See DOI: 10.1039/cXsm00000x/

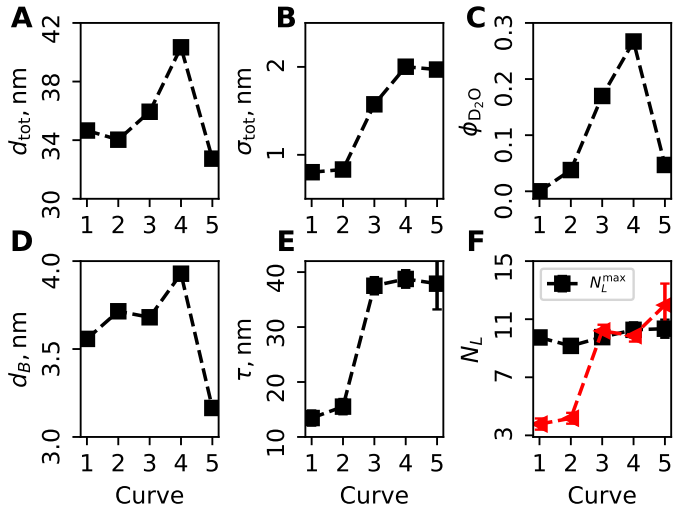

Fig. 2 Macroscopic parameters of the film. A. Total thickness of the film d_{tot}, determined by fitting the low-q part of the reflectivity curve.; B. Total roughness of the film σ_{tot}; C. Volume fraction of solvent $\phi_{\mathrm{D_2O}}$; D. d-spacing d_{B}, determined form the Bragg peak fitting.; E. Coherence length τ, determined from the width of the Bragg peak.; F. Black squares: maximum number of bilayers $N_{\mathrm{L}}^{\mathrm{max}}$ and red triangles: number of ordered layers in the coherent length N_{L}

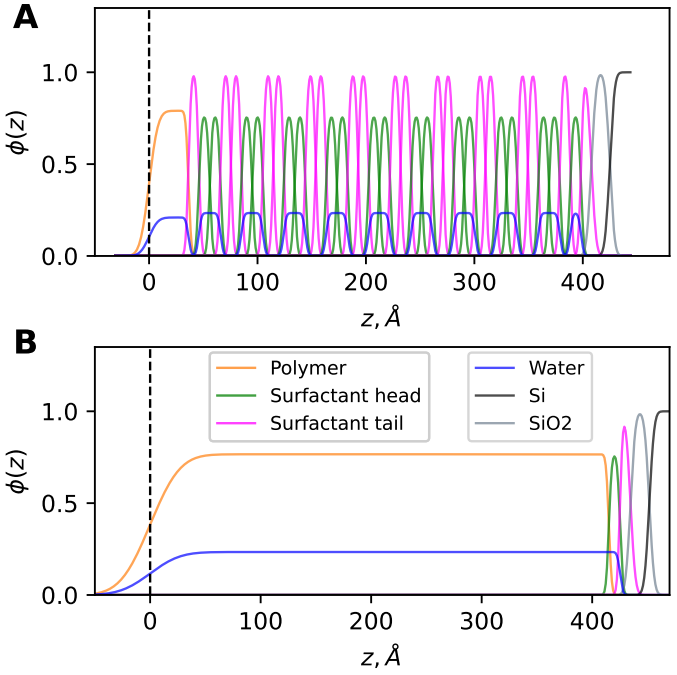

Fig. 3 Volume fraction distribution of the components in the A. Multilayer part of the film; B. Uniform part of the film. Dark gray line represents the Si substrate, light gray lines represents SiO2 layer, magenta lines represent hydrophobic domains, green lines represent hydrophilic domains, orange line represents polymer layer, blue line corresponds to the volume fraction of the solvent.

peak was less pronounced compared the h-surfactant film.

Upon increase in the RH, the Bragg peak shifted from $q = 0.175 \pm 0.001\,\text{Å}^{-1}$ in dry N2, towards lower q-values, as indicated in the Table **??**, indicating an increase in the multilayer d-spacing and swelling of the film. This was accompanied by the decrease in the width of the Bragg peak, indicating the increase in the average size of coherently scattering domain, i.e. the number of ordered layers in the multilayer increased. Concurrently, the Bragg peak intensity increased with the RH for both contrasts, although to a lesser extent for the films containing d-surfactants.

Fitting measured reflectivity in the low-q region ($q \leq 0.1^{-1}$) to the model of a uniform layer yielded the thickness d_{tot} and volume fraction of the solvent ϕ_{D_2O} in the film, assuming a uniform distribution of the polymer, surfactant and the solvent. Furthermore, fitting the Bragg peak to the Gaussian profile gave the centre position q_{B} and the width w_{B}. These values were used to calculate the d-spacing as $d_{\mathrm{B}} = 2\pi/q_{\mathrm{B}}$ and coherence length perpendicular to the substrate as $\tau = 2\pi/(2.355 \cdot w_{\mathrm{B}})$, where 2.355 is a full width at half maximum (FWHM) factor. Maximum number of layer was calculated as $N_L^{\mathrm{max}} = d_{\mathrm{tot}}/d_{\mathrm{B}}$. Macroscopic parameters of the film are shown in the Figure 2.

First, the Bragg peak analysis gives the d-spacing under dry N2 as $q = 0.177\,\text{Å}^{-1}$ with a coherence length $\tau = 13.44 \pm 1.37\,\text{nm}$, corresponding to $N_{\mathrm{L}} = 3.78 \pm 0.39 \simeq 4$ ordered bilayers, whereas the total film thickness $d_{\mathrm{tot}} = 34.66\,\text{nm}$ nm would accommodate up to 10 bilayers, as indicated by $N_L^{\mathrm{max}} = 9.74 \pm 0.23$. Upon exposure to humidity the Bragg peak width decreases, indicating an increase in the coherence length. As indicated in the Figure 2F, the maximum number of bilayers in the film remains almost constant, even though the total film thickness changes significantly, with increase of $\frac{d_{\mathrm{tot}}^{RH=80} - d_{\mathrm{tot}}^{RH=0}}{d_{\mathrm{tot}}^{RH=0}} = 16.4\%$, corresponding to the difference between "as-prepared" film and swollen at 80% relative humidity.

Additionally, exposure to humidity leads to the reversible change in the total film thickness d_{tot}, albeit with higher roughness, as evident from the Figures 2A and 2B.

Additionally, for reflectivities recorded at high humidity reflected intensity was calculated as an incoherent sum of the reflectivities from two different structures: a structure containing a multilayer and a uniform film with one wetting layer of the surfactant near the substrate. Coverage of the each component of the film was allowed to vary, so that the scaling coefficients add up to unity. Models, containing only multilayer structures did not produce good fits to the specular reflectivity profile at high humidity. Subsequently, fitted model was reconstructed to extract the volume fraction profiles of film components. as shown in the Figure 3A for the multilayer structure and Figure 3B for uniform layer at RH = 80 %.

As shown in the Figure 3A, the periodic part of the film contains 9 periodic repeat units and one monolayer of the surfactant near the substrate. Thickness of the bottom surfactant monolayer is allowed to be varied independently. Figure 3B corresponds to the distribution of components in the structure, containing uniform film. The difference in the total film thickness between the periodic and uniform part is about 35 Å and is partially compensated by the increase in total roughness of the uniform part, as compared to the periodic part.

Resulting fits are shown in the Figure 1. Models were highly constrained, however main features of the reflectivity curve, such as position of the critical angle, position of the Kiessig fringes and Bragg peak position, width and intensity are reproduced. It

should be noted, that some features are more pronounced in the model, but not visible in the data. This is due to the inhomogeneities in the illuminated area of the film (ca. 80 cm^2) not taken into account.

Additionally, the difference between the model and experimental data for the "as-prepared" film containing h-C12-AO is attributed to the non-completed exchange of the labile protons in the film, which can slightly distort the apparent SLD of the film.

1.2 Lateral organization of the film

The layered structure of the film is further confirmed by the presence of off-specular scattering, contributing to the appearance of a Bragg sheet at an angle to the specular reflectivity, as shown in the Figure 4A, indicating the presence of the lateral periodicity, or so-called roughness correlation [1,2].

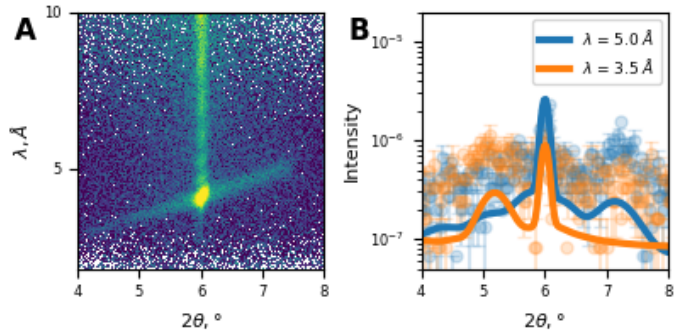

Fig. 4 Off-specular neutron reflectivity at high-q. A: h-contrast, experiment, B: h-contrast, cuts at $\lambda = 5$ Å and $\lambda = 3.5$ Å

Using the distorted-wave Born approximation (DWBA) and assuming correlated roughness for the multilayer model with full out-of-plane correlation between the layers it is possible to calculate the off-specular scattering signal. [3] Applying the model of in-plane correlations produced by thermally excited capillary waves and bending modes, resulting in two characteristic length scales ξ_1 and ξ_2. Analysis of the Bragg sheet scattering allowed the determination $\xi_1 = 150 \pm 30$ nm and $\xi_2 = 50 \pm 30$ nm, indicating bilayers with the ratio $\frac{\gamma}{\kappa} = 3.6 \cdot 10^{-3}$. Assuming the surface tension between the hydrated film and the Si wafer $\gamma_{FS} = 40$mN/m, it is possible to estimate bending modulus $\kappa = 22$ kT.

The calculations, as shown in the Figure 4B show good qualitative agreement between the measured (circles) and calculated intensity (solid lines) on the detector. Two dimensional simulated images can be found in the Figure **??**. The only significant difference is that the intensity of the simulated Bragg sheet is lower than the experimental intensity. This is explained by the fact, that the roughness is underestimated in the model. However, inclusion of higher roughness between the layer leads to the subsequent increase in the scattering length density contrast between the layers up to unphysical values. Value of roughness is important only for the overall intensity of the Bragg sheet, but the shape, which is determined by the values of the correlation lengths ξ_1 and ξ_2, is in good agreement with the experiment.

Measurements of the off-specular scattering at low-q, as shown in Figure 5A (h-contrast) and 5C (d-contrast) revealed the presence of the Yoneda scattering at $q < q_c$, which is due to the inhomogeneities in the film.

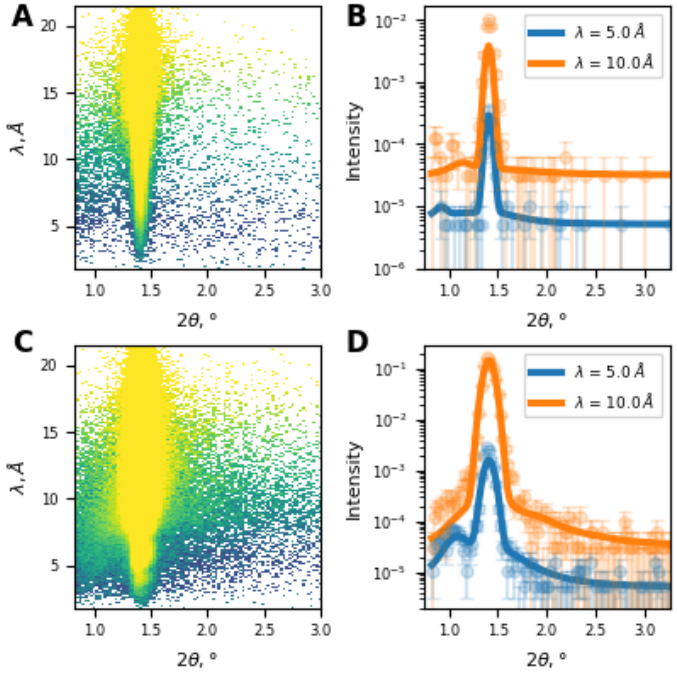

Fig. 5 Off-specular neutron reflectivity. A: h-contrast, experiment, B: h-contrast, cuts at $\lambda = 5$ Å and $\lambda = 10$ Å, solid lines are calculated fits according to the model, described in the text ,C: d-contrast, experiment, D: d-contrast, cuts at $\lambda = 5$ Å and $\lambda = 10$ Å, solid lines are calculated fits according to the model, described in the text.

Yoneda scattering was calculated using the DWBA approximation and comparison with the experiment is shown in the Figure 5B and 5D with the line cuts at different wavelengths. The model was built using a uniform layer with shallow cylindrical pores located on the surface of the film. The radius of the pores was found to be $R = 900$ nm and the depth $d = 2.5$ nm.

We acknowledge beam time allocation on FIGARO at ILL (http://doi.ill.fr/10.5291/ILL-DATA.9-12-669).

Notes and references

1 T. Salditt, T. H. Metzger and J. Peisl, *Physical Review Letters*, 1994, **73**, 2228–2231.

2 Z. X. Li, J. R. Lu, R. K. Thomas, A. Weller, J. Penfold, J. R. Webster, D. S. Sivia and A. R. Rennie, *Langmuir*, 2001, **17**, 5858–5864.

3 A. Hafner, P. Gutfreund, B. P. Toperverg, A. O. F. Jones, J. P. d. Silva, A. Wildes, H. E. Fischer, M. Geoghegan and M. Sferrazza, *Journal of Applied Crystallography*, 2021, **54**, 924–948.